Drainage Canals in Southeast Asian Peatlands Increase Carbon Emissions

Nathan C Dadap[1], Alison M Hoyt[2,3], Alexander R Cobb[4], Doruk Oner[5], Mateusz Kozinski[5], Pascal V Fua[5], Krishna Rao[1], Charles F Harvey[6], and Alexandra G Konings[1]

[1] Department of Earth System Science, Stanford University, Stanford, CA
[2] Max Planck Institute for Biogeochemistry, Jena, Germany
[3] Lawrence Berkeley National Laboratory, Berkeley, CA
[4] Center for Environmental Sensing and Modeling, Singapore-MIT Alliance for Research and Technology, Singapore, Singapore
[5] École Polytechnique Fédérale de Lausanne, Lausanne, Switzerland
[6] Department of Civil and Environmental Engineering, Massachusetts Institute of Technology, Cambridge, MA

Corresponding author: Nathan C. Dadap (ndadap@stanford.edu)

Key Points

- We created the first map of drainage canals across Southeast Asian peatlands and find that they are present across 65% of the region.
- There is substantial variation in drainage density within land use types, indicating that land use is a poor proxy for drainage.
- Peat carbon emissions associated with subsidence are higher in areas with progressively more drainage canals.
-

Abstract

Drainage canals associated with logging and agriculture dry out organic soils in tropical peatlands, thereby threatening the viability of long-term carbon stores due to increased emissions from decomposition, fire, and fluvial transport. In Southeast Asian peatlands, which have experienced decades of land use change, the exact extent and spatial distribution of drainage canals are unknown. This has prevented regional-scale investigation of the relationships between drainage, land use, and carbon emissions. Here, we create the first regional map of drainage canals using high resolution satellite imagery and a convolutional neural network. We find that drainage is widespread – occurring in at least 65% of peatlands and across all land use types. Although previous estimates of peatland carbon emissions have relied on land use as a proxy for drainage, our maps show substantial variation in drainage density within land use types. Subsidence rates, and corresponding carbon losses from decomposition, are 3.2 times larger in intensively drained areas than in non-drained areas, highlighting the central role of drainage in mediating peat carbon fluxes. Accounting for drainage canals was found to improve a subsidence prediction model by 30%, suggesting that canals contain information about subsidence not captured by land use alone. Thus, our dataset can be used to improve carbon emissions predictions in peatlands and to target areas for hydrologic restoration.

Plain Language Summary

Tropical peatlands are swamp-like environments in which naturally wet conditions slow the decomposition of plant carbon that would otherwise be released to the atmosphere. However, over the past few decades, humans have built drainage canals in Southeast Asian peatlands, due to economic pressure for logging and agriculture. These canals are a major threat to peatlands because they dry out peat soils, in turn speeding up decomposition and making soils susceptible to wildfire. Both of these mechanisms release massive amounts of carbon dioxide to the atmosphere, thereby accelerating climate change. Despite these risks, until now the extent of drainage in peatlands was unknown due to a lack of drainage canal maps. Here, we create the first regional map of drainage canals by training a computer algorithm to identify canals within high-resolution satellite images. We find that drainage is widespread – occurring in at least 65% of Southeast Asian peatlands. Furthermore, we find that more drainage canals are related to progressively larger emissions of carbon dioxide to the atmosphere. These findings suggest that it is important to know where and how much drainage is occurring to accurately predict carbon dioxide emissions and target areas for restoration.

1 Introduction

Hydrology governs carbon storage dynamics in tropical peatlands (Cobb et al., 2017; Dommain et al., 2010; Hirano et al., 2009). In these wetland environments, persistent flooding and anoxic conditions suppress decomposition rates, allowing organic material to accumulate over time in deep peat deposits. This process, compounded over millennia, has made Southeast Asian (SEA) peatlands one of the world's largest terrestrial pools of organic carbon: an estimated 67 Gt of carbon are stored in peatlands in Indonesia, Malaysia, and Brunei (Page et al., 2011; Warren et al., 2017). In recent decades, this carbon sink has been threatened by human disturbance (Leifeld & Menichetti, 2018). Widespread deforestation and conversion of peat swamp forests for agricultural use since the 1980's have left only ~6% of primary forests intact (Miettinen et al., 2016). Just as importantly, drainage canals constructed for transporting forestry products and improving agricultural yields (Bader et al., 2018) directly impact local hydrology by lowering water tables (Hooijer et al., 2010; Lim et al., 2012).

Hydrologic changes in peatlands have the potential to destabilize long-term peat carbon stocks, resulting in considerable carbon emissions. In situ studies measuring soil CO_2 flux found that decomposition rates are closely linked to water table depth (e.g., (Hirano et al., 2009; Hoyt et al., 2019; Jauhiainen et al., 2005)). As soils dry out, aerobic respiration increases, in turn causing higher CO_2 fluxes that result in peatland subsidence (Couwenberg et al., 2010; Hooijer et al., 2012; Jauhiainen et al., 2012). These potential emissions are substantial, as a recent study estimated that tropical peatland emissions due to drainage may comprise over 1/3 of the greenhouse gas budget for keeping global temperature rise below 2 °C (Leifeld et al., 2019). Peat fires, which also release massive amounts of carbon dioxide (Page et al., 2002) and cause regional haze events with widespread human health effects (Koplitz et al., 2016), have grown in recent decades, indicating that drainage is drying out peatlands on a large scale (Dadap et al., 2019; Field et al., 2009). Furthermore, drainage canals increase fluvial export of dissolved organic carbon (Gandois et al., 2020; Moore et al., 2013).

Drainage of peatlands drives each of the regions' major carbon emissions mechanisms. However, the extent, distribution, and spatial patterns of drainage canals are unknown. As a result, all recent studies estimating regional carbon emissions have instead relied on emissions factors based on land use and land cover type (e.g., (Carlson et al., 2013; Hiraishi et al., 2014; Leifeld & Menichetti, 2018; Miettinen et al., 2017; Murdiyarso et al., 2010)). Such estimates implicitly rely on the assumption that drainage characteristics are linked to land use type. However, land use classifications neglect differences in drainage practices (e.g. prevalence of drainage canals, canal and water table depth, canal maintenance, etc.) that may vary widely within a given land use class. Consequently, the use of land use-based emissions factors to estimate carbon emissions and peatland subsidence at larger scales may introduce significant inaccuracies.

Here, we address these gaps by answering three central questions regarding hydrologic disturbance in SEA peatlands: 1) How widespread are drainage canals? 2) How does drainage differ between land use classes? and 3) Does drainage predict subsidence from peat oxidation at large scales? To answer these questions, we created the first region-wide, high-resolution (5 m) map of drainage canals in SEA peatlands, then compared drainage canal density to land use and subsidence data. We found that drainage is widespread and that drainage varies considerably within land use types. Carbon fluxes associated with peat subsidence are higher in areas with progressively higher drainage canal density throughout the region. Furthermore, accounting for drainage canals was found to substantially improve a subsidence prediction model, suggesting that canals contain information about subsidence not captured by land use alone.

2 Data and Methods

2.1 Development of drainage canal and drainage density maps

We mapped drainage canals across SEA peatlands, an area that encompasses 157,000 km^2 on the islands of Sumatra and Borneo, and on Peninsular Malaysia (approximately 6°S to 6°N and 95°E to 120°E). This region is estimated to contain ~65% of all soil carbon stored in tropical peatlands (Page et al., 2011; Warren et al., 2017). In addition to 5 m resolution maps of drainage canals, we also created a second map depicting drainage density at 1 km resolution, defined here and throughout the manuscript as the length of drainage canals per unit area (in units of km/km^2). We chose 1 km resolution for mapping drainage density because it is sufficiently coarse to reduce noise in the 5 m canal map but fine enough to capture land use features in this region.

2.1.1 Satellite imagery

To create the drainage canal map, we trained a model to identify canals within high-resolution satellite images from 2017 produced by Planet Labs, Inc. (“Planet”) (Planet Team, 2017). This dataset has wall-to-wall coverage throughout the study area at high, 5 meter resolution. Here, we used the “global_quarterly_2017q3_mosaic Basemap” product, which is a global mosaic of RGB images taken by the PlanetScope constellation of CubeSat sensors between July and September 2017. This dataset has two salient features that make it well-suited for the canal classification task. First, it has high – 5 meter – resolution that is necessary (Wedeux et al., 2020) for identifying narrow drainage canals that can be just meters in width (Evans et al., 2019; Jauhiainen & Silvennoinen, 2012). Secondly, this dataset exhibits very low cloud cover because Planet’s mosaicking algorithm layers images according to a ranking of image quality based on cloud cover and sharpness. The July-September time period was selected because it coincides with the SEA dry season (Aldrian & Dwi Susanto, 2003), further reducing cloud contamination in the dataset. The Basemap data was used without further correction or alteration.

2.1.2 Training, validation, and test data

To our knowledge, there are no publically available drainage canal maps in the study area that could be used for model development with complete and correct data, as well as accurate georeferencing to within a few meters. Even at the sub-regional scale, such maps are not available. Some hand-labeled canals are delineated in Open Street Maps, but these data appear to be intermittent and of unknown origin and accuracy, likely due to the fact that labeled data on that platform are open source and contributor-driven. Thus, it is difficult to gauge the accuracy, completeness, and possible biases in the data, and cannot be easily used for scientific research on drainage extent. Instead, we generated training, validation, and test data by manually labeling the Planet Basemap satellite images (Fig. 1). This process was performed in Google Earth Engine (Gorelick et al., 2017) by hand-tracing canals with line vectors, then extruding them to create a raster image of canal labels. We also labeled roads as canals because roads are commonly accompanied by drainage ditches and/or may inadvertently result in peatland drainage (Lim et al., 2012; Miettinen et al., 2012). In total, the labeled imagery spans ~2500 km^2 across multiple land use types in the Bengkalis and Siak Regencies in Riau Province, Sumatra, Indonesia.

We also labeled images to generate validation and test datasets for assessing out-of-sample accuracy (Figures S1 and S2 in the Supporting Information). Test data differs from the validation data in that it was labeled by an independent labeler, allowing for an assessment of potential systematic bias from human labeling error. The validation area were comprised of ~100 km^2 or 4% of the labeled data in Riau, and were selected to span multiple land use types and drainage densities. Test data locations were selected for four areas spread across the study area, chosen via stratified random sampling (Figure S2).

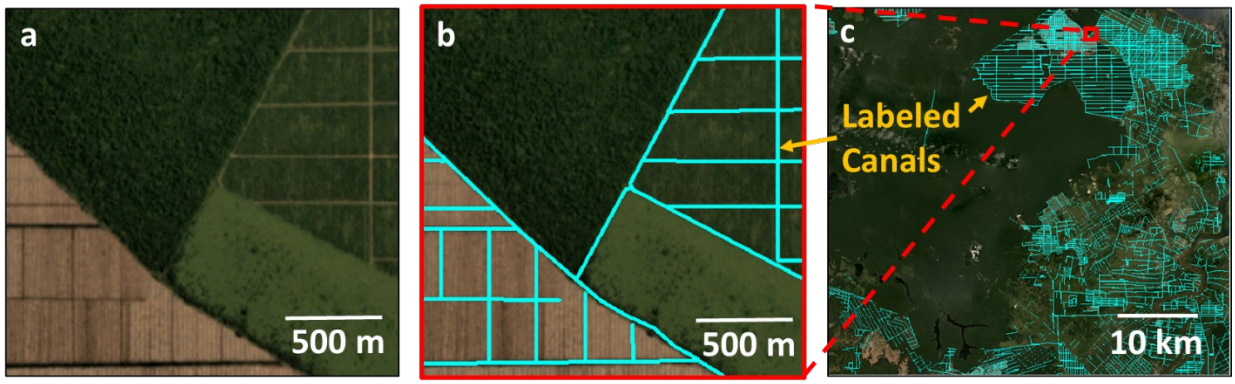

Figure 1. Training data for canal classification. a) Example of 5 meter resolution Planet Basemaps imagery used for identifying drainage canals. **b)** Hand-labeled canals in turquoise overlay example image. **c)** Full training dataset in Riau Province, Sumatra, Indonesia. Training area (~2,500 km^2) spans all land use types and a wide range of canal densities.

2.1.3 Classification Methodology

A convolutional neural network (CNN) was used to identify drainage canals within the satellite imagery. Originally developed in the context of handwriting recognition (LeCun et al., 1998), CNNs have seen an increase in usage since 2012, when they were shown to achieve superior performance in image classification tasks (Krizhevsky et al., 2017). Pixel by pixel classification schemes fail at identifying drainage canals in images because canals exhibit variable radiative spectral signatures; canals can be covered by open water, soil, or vegetation

when covered by canopy or overgrown brush. Thus, the ability of CNNs to consider the context around a pixel to identify linear shapes is of paramount importance for canal identification. We further used a state of the art canal-segmentation algorithm that was originally designed to identify roads from satellite imagery (Oner et al., *under review*) because canals, like roads, are narrow linear features of varying width. This algorithm uses a recurrent CNN with U-Net architecture (Ronneberger et al., 2015), and incorporates in its objective function loss terms that promote global connectivity. As a result, it outperforms other state-of-the-art methods and we refer the interested reader to Oner et al. (*under review*) for more details.

2.1.4 Model Assessment

We assessed canal map accuracy using the quality metric, which is defined as the number of true positives divided by the sum of true positives, false positives, and false negatives. This metric is commonly used in road mapping classification, and is more appropriate than the accuracy metric (defined as the number of true positives divided by the sum of true positives, true negatives, false positives, and false negatives) due to a high number of true non-canal pixels (Wiedemann et al., 1998). As noted in Oner et al. (*under review*), the definition of a true positive was relaxed to allow for positive matches within a distance of 5 pixels, to avoid penalizing the results for minor spatial mismatches in canal location. We also evaluated the accuracy of drainage density measurements by calculating the squared Pearson correlation coefficient (r^2), root-mean-squared-error (RMSE), and bias between retrieved drainage density data to validation and test datasets at 1 km resolution. While classification results would ideally be compared to an independent "true" dataset that is based on ground-truthed data of canal locations, such a dataset does not exist in this region. As such, manually-labeled satellite images are currently the best method for generating training and validation data for canal mapping.

2.2 Land Use Analyses

To better understand the relationship between drainage and land use, we compared drainage density to land use data obtained from maps by Miettinen et al. (2016), which are based on hand-delineation of 2015 Landsat images. Our analyses were conducted at 1 km resolution to match the selected resolution of our drainage density map. We filtered out pixels where the most common land use type did not constitute an absolute majority of the pixel. In accordance with the changes in land use classes applied by Miettinen et al. (2017), the 'Seasonal water', 'Ferns/low shrub' and 'Clearance' categories were combined under the 'Open undeveloped' designation, to better reflect land use classes used in IPCC emissions factors. Drainage density categories were defined by binning drainage density values into 4 classes, as shown in Equation 1. Examples of canal networks based on these drainage density categories are shown in Fig. 4 and Figure S3.

$$\textit{Drainage density category} = ¿ \quad (1)$$

2.3 Subsidence analyses

We analyzed the relationship between drainage and subsidence by comparing to data from Hoyt et al. (2020), who measured subsidence across eight 100 x 100 km frames in the study area. These data were measured using interferometric synthetic aperture radar (InSAR) data from Japan Aerospace Exploration Agency's Advanced Land Observing Satellite (ALOS-1), and are

the only subsidence measurements in SEA peatlands available over a large area. InSAR-based subsidence measurement involves measuring phase changes in the reflected radar beam between subsequent passes of an observing satellite, allowing for millimeter-scale sensitivity to changes in elevation. We estimated the associated carbon fluxes from the subsidence data using the approach outlined by Hoyt et al. (2020), as described further in Text S1 of the Supporting Information. Note that these data represent the period 2007-2011, 6-10 years before the drainage estimates.

We plotted probability distributions of subsidence as grouped by drainage density using kernel density estimation. The median subsidence and standard error were then calculated for each distribution. An independent sample T-test without assumption of equal variance was applied to each pair of distributions; p-values $<<0.01$ for all combinations imply that the difference in mean subsidence between all drainage groups is statistically significant. Due to the ~8 year temporal mismatch between the subsidence and drainage density datasets, we present results only for areas where land use change did not occur between 2007 and 2015; however inclusion of those areas did not significantly change the results.

We further assessed the value of drainage metrics in predicting subsidence by creating a random forest model for subsidence, then evaluating the increase in model explanatory skill (as calculated by the coefficient of determination R^2) when including drainage metrics. The non-drainage predictor features used were land use type and distance to peat edge – two features that were previously used to predict subsidence at regional scales (Hoyt et al., 2020) – and active fire count, which was assumed to contain information regarding the hydrologic state of a given area. The drainage metrics used were drainage density (with continuous values, rather than discretized by categories) and average distance to canals. Both were calculated at 1 km resolution from the 5 m resolution canal map. Although drainage density and distance to canals have an inverse relationship (Figure S4), it is not exactly one-to-one, depending on the details of the canal geometry in a given location. Furthermore, distance to canals is a potentially more informative predictor of subsidence (relative to drainage density alone), since it is expected to more closely match the effect of canals on nearby water table depths than drainage density alone (Sinclair et al., 2020). Thus, we chose to include both drainage metrics in the model. Additional details on the development of the random forest subsidence model are provided in Text S2 of the Supporting Information.

3 Results

3.1 Canal classification accuracy

Our canal classification map exhibits high accuracy in the validation and test areas. Visual inspection of the 5 m resolution canal map show that the classification captures the overall spatial patterns of drainage canals (Figures S1 and S2). The dataset displays a quality score of 0.85 in the validation area, a value that compares favorably to recent road mapping efforts (Oner et al., *under review*). Because traditional binary classification metrics are highly imbalanced for canal maps (since most pixels are non-canals), we also assessed model performance on drainage density data aggregated to 1 km x 1 km resolution. To make this comparison, we created a map of drainage density (Methods, Fig. 3a). Drainage density results in the validation area displayed high correlation with hand-labeled drainage density data (r^2=0.89, RMSE = 0.77 km/km^2) and were slightly conservative (underestimation of drainage density with

bias = -0.47 km/km^2 vs. mean 3.08 km/km^2; Fig. 2a). A comparison to a separate test dataset was also performed; the test data differs from the validation data in that it was labeled by an independent labeler, allowing for an assessment of potential systematic bias from human labeling error. Similar performance between the validation and test results (r^2=0.83, RMSE=1.3 km/km^2, bias = -0.85 km/km^2; Fig. 2b) suggest that there is no significant bias in the results due to labeling error.

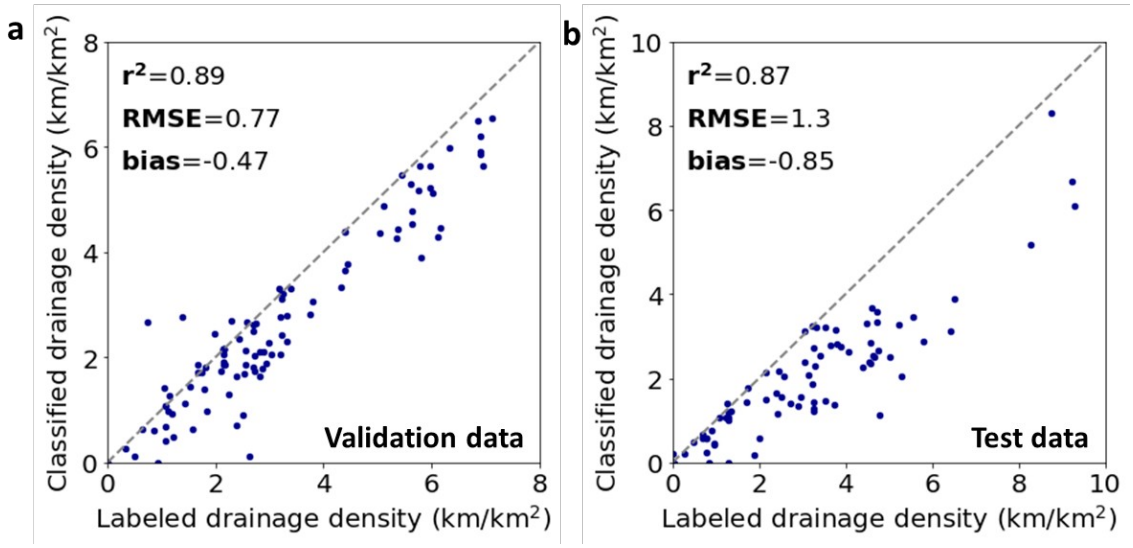

Figure 2. Canal classification performance. Scatterplots showing drainage density of classified canals vs drainage density of labeled canals in a) validation and b) test areas.

3.2 Extensive drainage in SEA peatlands

Our drainage density map (Fig. 3a) reveals that drainage is widespread: 65% of 1 km x 1 km pixels (spanning 93,000 km^2) in SEA peatlands were found to contain drainage canals. Given the 5 m resolution of the input images, these results pertain only to canals ≥ 5 m width. The omission of narrow canals, in addition to the fact that the model exhibits negative bias, suggest that the true percentage of drained peatlands is likely even higher than the 65% estimate determined here.

There are notable spatial patterns of drainage density within the drainage canal maps (Fig. 3b and 2c). For example, in northern Borneo, there is an abrupt shift in drainage density across the border between Malaysia and Brunei, corresponding to differences between plantations and conservation areas in each of the two countries. Similarly, areas in Central Kalimantan within the ex-Mega Rice Project area (much of which underwent extensive drainage in the 1990's (Houterman & Ritzema, 2009)) still exhibit higher drainage densities than in the adjacent and relatively protected Sebangau National Park, which has little drainage. Accordingly, this map of drainage density (Fig. 3a) and the 5 m resolution canal map (examples shown in Fig. 3b and 3c) depict varying degrees of peatland hydrologic disturbance.

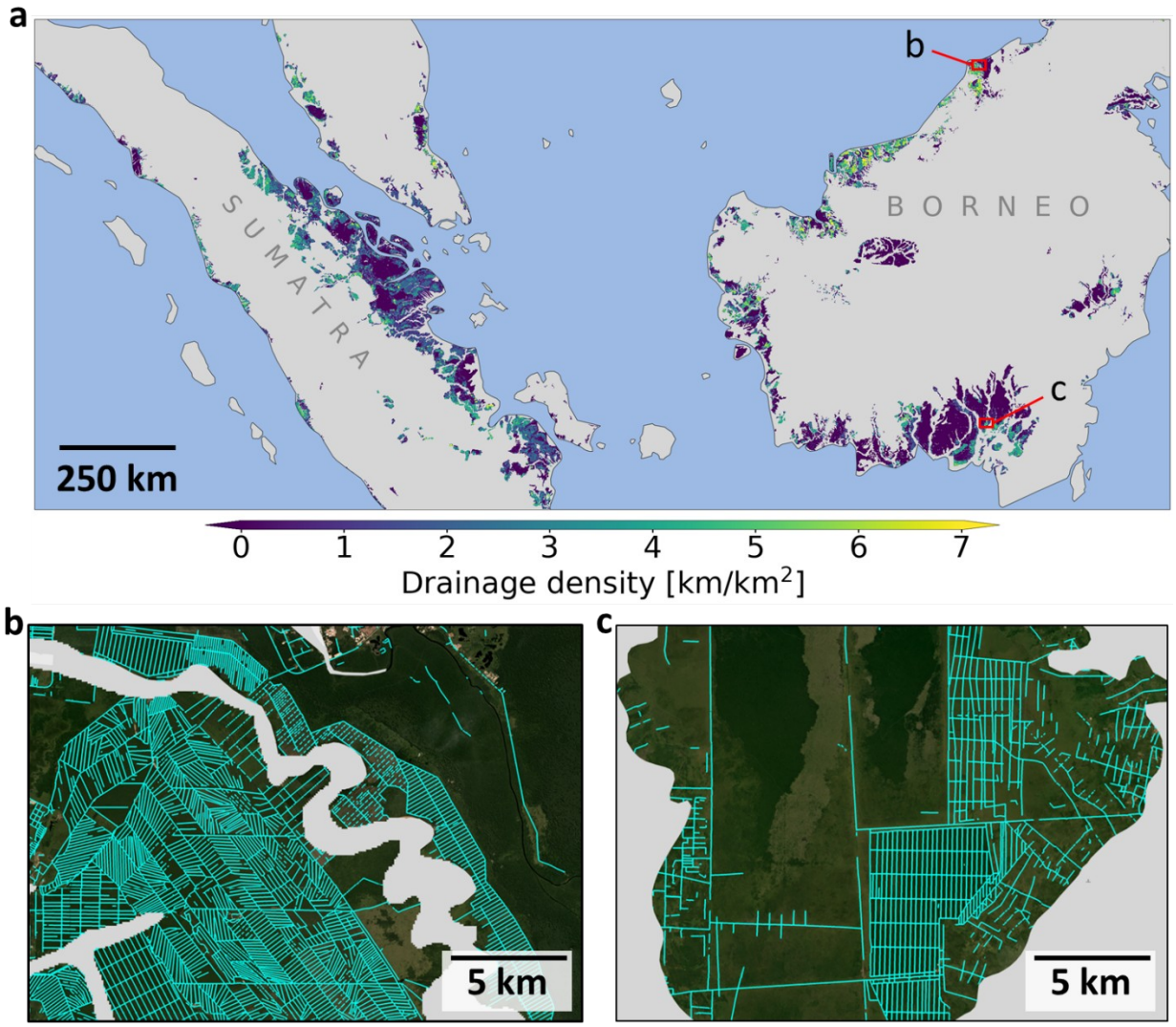

Figure 3. Canal classification results. **a)** Map of drainage density [canal length per peat area, km/km^2] across SEA peatlands at 1 km resolution as retrieved from 2017 satellite imagery. Non-peatland areas are shown in gray. Red boxes outline example areas showing 5 m resolution canal maps in **b)** Sarawak, Malaysia / Belait, Brunei and **c)** Block B of the former Mega Rice Project area in Central Kalimantan, Indonesia.

For subsequent analyses, we grouped the data into drainage density categories to reduce the sensitivity of our results to classification error. These encompass categories of None (no canals detected), Low (0 – 2.5 km/km^2), Moderate (2.5 – 5 km/km^2), and High (>5 km/km^2) drainage density. To illustrate these categories, examples of the spatial pattern of canals underlying each category are shown in Fig. 4 and Figure S3. Areas with High or Moderate drainage density are generally indicative of dense, systematic drainage networks and account for 37% (~36,000 km^2) of all drained peatlands.

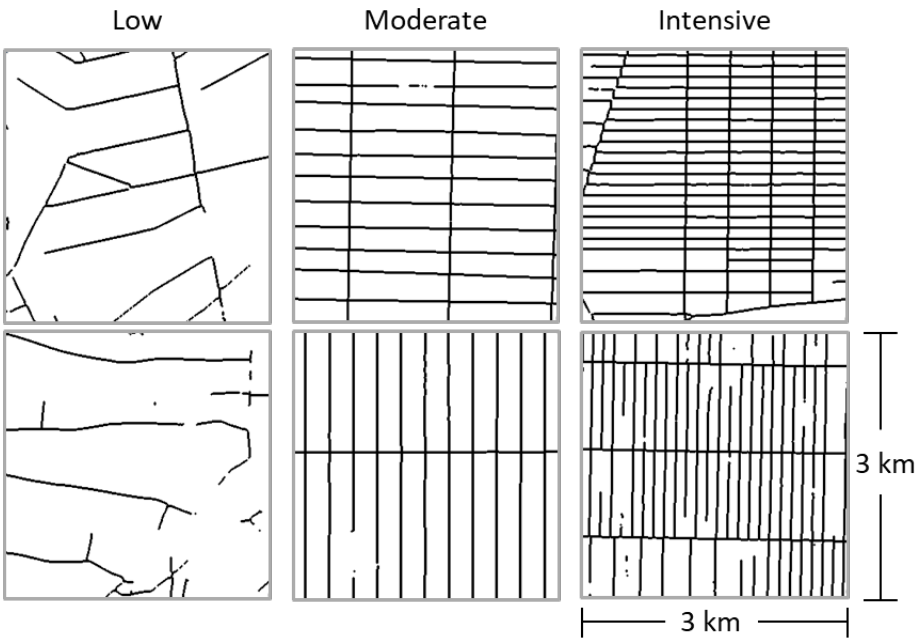

Figure 4. Examples of drainage density categories. Classified canals (black) are shown in 3 km x 3 km squares, sorted by drainage density categories in each column. Examples were selected from areas in Sarawak, Malaysia and West Kalimantan, Indonesia. Drainage density categories of Low, Moderate, and High drainage correspond to drainage densities of 0 - 2.5, 2.5 - 5, and > 5 km / km^2. Additional category examples are shown in Figure S3.

3.2 Drainage density varies within land use types

Across all of the major land use categories considered, except pristine forests, there is substantial variation in drainage density. For example, in industrial plantations, Moderate drainage density occurs in 51% of plantations and Low drainage density in 34% (Fig. 5a). Similarly, areas classified as smallholder plantations, open undeveloped, and degraded forest areas also exhibit considerable variation in drainage density, with each of these land use types containing at least two drainage density categories that span 15% of its area or more. Overall, the variation in drainage density within each land use type (Fig. 5a) indicates that land use classifications alone are insufficient to capture hydrologic impacts from drainage canals in SEA peatlands.

Drainage density is generally higher in industrial and smallholder plantations than in pristine forest, degraded forest, or open undeveloped areas. Plantations comprise 91% of areas that have High or Moderate drainage density, and industrial plantations make up 75% of those categories alone. In contrast, areas with Low drainage density are more evenly distributed between smallholder plantations (42%), industrial plantations (24%), open undeveloped (18%), and degraded forest (13%) land use types (Fig. 5b). Although considerable peatland management efforts and regulation have been focused on drainage in industrial plantations, they comprise only 43% of the total drained area.

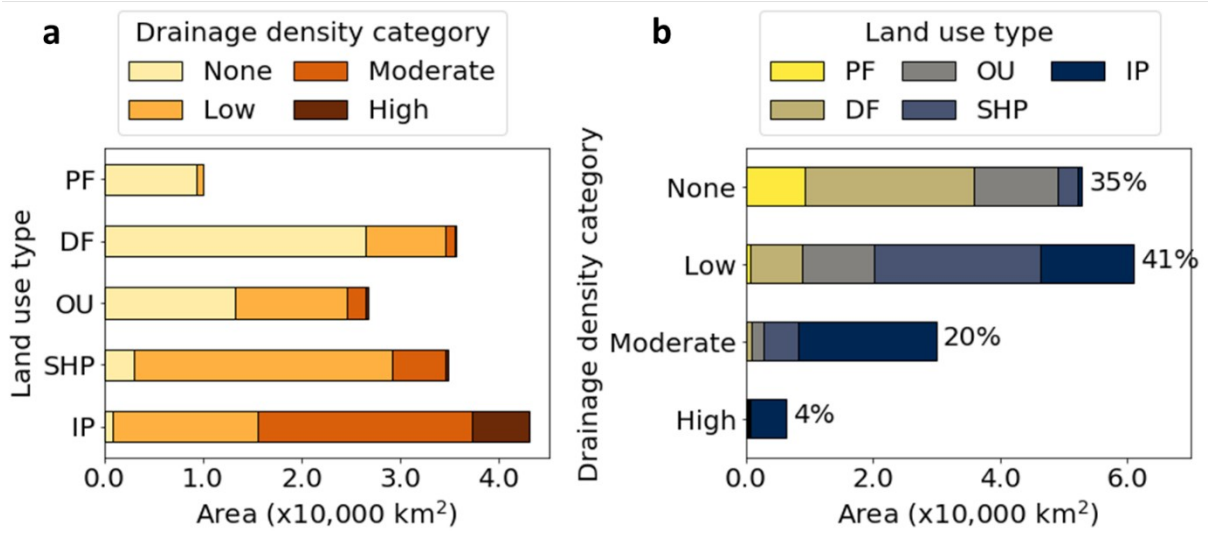

Figure 5. Distribution of drainage density in peatlands. a) Land use types are subdivided by drainage density categories, defined as None (no detected canals), Low (0 - 2.5 km/km^2), Moderate (2.5-5 km/km^2), and High drainage (> 5km/km^2). PF denotes pristine forest, DF- degraded forest, OU- open undeveloped, SHP- smallholder plantation, and IP- industrial plantation. **b)** Drainage density categories are subdivided by land use type. The percent of total peatland area for a given drainage density is shown next to the bar.

3.3 Drainage density predicts subsidence and peat carbon fluxes

In mapping peatland drainage across the region for the first time, we find that subsidence rates (a measure of carbon emissions) are higher in areas with progressively higher drainage density. To assess the effect of drainage on carbon fluxes, we compared drainage density to subsidence rates measured from 2007-2011 (Hoyt et al., 2020), and found that High drainage density areas have median subsidence rates that are 1.3x larger than in Moderate drainage density areas, 1.5x larger than in Low drainage density areas, and 3.2x larger than in areas with no drainage (Fig. 6). This relationship holds even though drainage density data were measured 8 years after the subsidence measurements. The positive relationship between drainage density and subsidence, although not always evident, can sometimes be observed visually in maps depicting subsidence and canals, with several examples shown in Figure S5. Median subsidence values are significantly different between classes (for t-tests applied to distribution means, $p<<0.01$). However, it should be noted that the relationship between drainage density and subsidence does not hold in the ex-Mega Rice Project area in Central Kalimantan, Indonesia (Figure S6), likely due to the presence of deeper drainage canals and deeper overall water table depths in that area (see Discussion). Across all other areas, pixels with high drainage density have subsidence rates that are 1.86 ± 0.09 cm/yr greater than in areas with no drainage. These differences in subsidence rates translate to significantly increased carbon fluxes, as CO_2 emissions can be estimated based on characteristics of the peat lost during subsidence (see Methods and Supporting Information). Assuming a mean peat carbon content of 55% and dry bulk density of 0.08 g/cm^3 (Couwenberg & Hooijer, 2013), the subsidence rate in intensively drained areas corresponds to 11.8 ± 1.9 tC/ha/yr of emissions, a large flux relative to the 3.6 ± 0.6 tC/ha/yr emissions rate in areas where drainage canals were not detected.

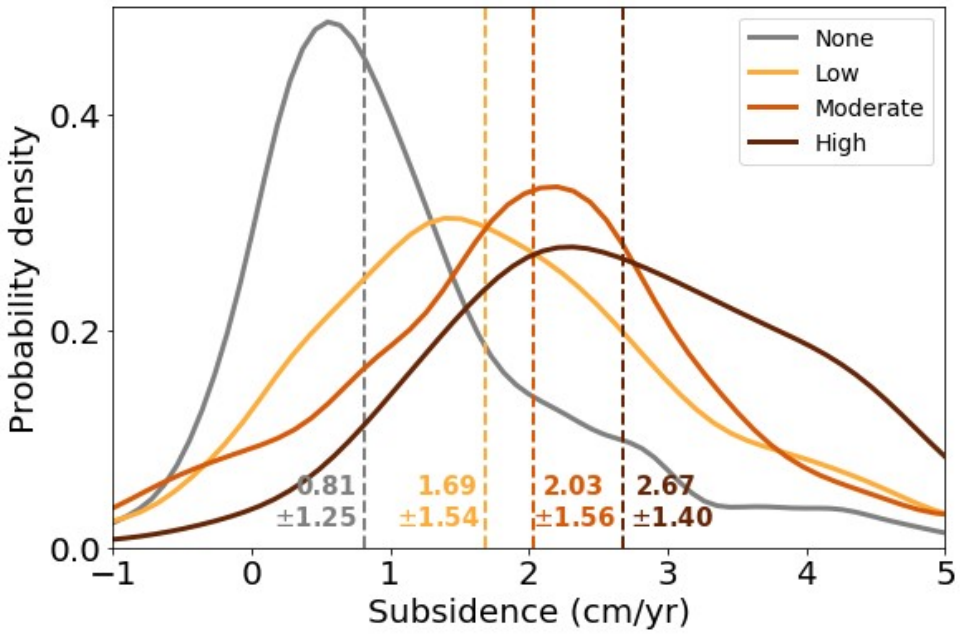

Figure 6. Relationship between subsidence and drainage density. Distribution of subsidence rates are shown for each drainage density category. Dashed vertical lines show medians for each distribution. Median ± standard deviation is shown for each distribution next to median line. Positive subsidence denotes downward ground surface displacement and CO_2 release to the atmosphere. Subsidence was measured by Hoyt et al. (2020) using ALOS-1 PALSAR interferometric data from 2007-2011.

Accounting for drainage canals substantially improved our ability to predict subsidence rates, suggesting that drainage maps contain important hydrologic information not captured by land use alone. Here, we built a random forest model of subsidence (at 1 km resolution), and assessed model performance when including drainage metric inputs. Addition of drainage metrics to a model with land use, distance to peat edge, and fire-related predictor variables increased the amount of explained variability in subsidence by 30% (from $R^2 = 0.3$ to R^2=0.39). Drainage metrics were the second most important category of information in the random forest model (Table S1), underscoring the importance of including canal-based drainage metrics in assessing peatland carbon emissions.

4 Discussion

4.1 Implications of widespread drainage

We created the first region-wide map of drainage canals and found that a majority of SEA peatlands are drained (Fig. 3a). This map makes it possible to disentangle drainage from land use. While most of the literature has focused on assessing impacts of drainage within the context of industrial plantations, we found that 57% of areas containing drainage canals (i.e., 57% of 1 km x 1 km tiles) are outside of industrial plantations, underscoring the importance of considering drainage impacts across all peatland land use types. Areas with Moderate and High drainage density are mainly comprised of industrial plantations, and areas with Low drainage density are primarily smallholder plantations. Land use has often been used to parameterize drainage in hydrologic models and for upscaling of carbon emissions estimates (e.g., (Mezbahuddin et al.,

2015; Miettinen et al., 2017; Taufik et al., 2020), and more). However, drainage density was found to vary within each land use type (Fig. 5a). This suggests that while drainage may convey information about possible land use types, particularly for high drainage densities (Fig. 5b), land use is a poor proxy for drainage in the region. Drainage metrics such as drainage density provide a means to compare hydrologic impacts at sub-regional scales even within homogenous land use types.

Drainage canals affect respiration rates via a hydrologic link: drainage lowers water tables and dries out peat soils, which in turn increase peat oxidation (Carlson et al., 2015; Couwenberg et al., 2010; Couwenberg & Hooijer, 2013; Hooijer et al., 2010, 2012; Jauhiainen et al., 2012). While these mechanisms have previously only been demonstrated at local scales, our results confirm the importance of these relationships at regional scales, as subsidence is found to vary with drainage density across the region (Fig. 6). This relationship holds despite a roughly 8 year difference between the subsidence dataset (measured from 2007-2011) and the drainage density dataset (2017) which likely adds noise to the relationship. Still, subsidence rates may be affected by land use change impacts apart from drainage. For example, non-drainage disturbances to peatlands include deforestation, use of fire to clear land, and conversion for agricultural use (Dohong et al., 2017). These disturbances, independent of drainage, may in turn cause secondary impacts to ecohydrological variables, such as water table depth (Hirano et al., 2009), soil physical properties such as bulk density, pore structure, and hydraulic conductivity (Kurnianto et al., 2018; Sinclair et al., 2020; Wells et al., 2016). They can also impactevapotranspiration due to shifts in photosynthetic rates and rooting depth (Hirano et al., 2015; Manoli et al., 2018). Such impacts may also partially explain why non-zero subsidence is evident in areas where drainage canals were not detected (Fig. 6). Secondary impacts of land use interact with those attributable to drainage, and a full assessment of the effects on subsidence would likely require the use of a hydrologic model. While such an analysis is beyond the scope of this study, we verified the utility of drainage metrics independent of land use using an empirical, random forest model for subsidence. When accounting for drainage metrics in the model that already accounted for land use, we found an improvement in model performance of 40% (Table S1), suggesting that drainage provides significant information about subsidence not captured in land use data alone. Thus, our results indicate that future estimates of peatland emissions from decomposition would benefit from inclusion of drainage metrics.

Drainage also increases peatland fire risk (van der Werf et al., 2008). In peatlands, organic soil is flammable if sufficiently dry, and only soil above the water table can catch fire (Usup et al., 2004). Accordingly, water tables lowered by drainage canals can increase the potential depth of peat fires and fire frequency (Konecny et al., 2016). Drainage impacts can extend beyond the areas adjacent to canals. For example, recent studies found that the presence of canals affected water table depths hundreds of meters away (Astiani et al., 2017; Evans et al., 2019) and forest biomass growth up to 1 km away (Wedeux et al., 2020). Accordingly, even isolated canals can have far-reaching hydrologic impacts via their impact on water tables in the surrounding area, underscoring the utility of their detection.

4.2 Beyond quantification of drainage density

The classification of narrow, linear features such as canals from satellite images requires high resolution imagery, and can only occur at the resolution of the input data. For example, recent attempts to identify logging canals in SEA found that canals were invisible using 30 m resolution Landsat images (Wedeux et al., 2020). Tree canopies can obscure narrow canals

(Jaenicke et al., 2010), but the 5 m resolution data used here allows for increased visibility of narrower canals through some vegetation cover. Nevertheless, 5 m resolution is still too coarse to consistently capture drainage canals <5 m in width, which also contribute to peatland hydrologic disturbance. Thus, classification performance may be disproportionately worse in land use types with more dense vegetation cover. Accordingly, we recommend that future efforts to map drainage canals use imagery at sub-1 m resolution where available. Information from additional sources (e.g. remote sensing images from different types of instruments) may also improve canal detection, and the deep learning model used here is flexible to allow for multiple input data sources. In particular, low frequency microwave observations that can penetrate vegetation could be promising for use in SEA peatlands (Dadap et al., 2019). However, the use of multiple sensors may also introduce georeferencing errors if there is any spatial mismatch between datasets. Ultimately, our validation results suggest that a single data source with 3 optical channels (red, green, and blue wavelength observations) was sufficient for classification of the >5 m canals identified here.

In contrast to the observed drainage-subsidence relationship (Fig. 6) that exists throughout a majority of the region, the ex-Mega Rice Project area in Central Kalimantan (Figure S6), exhibits high subsidence even in areas with low or no apparent drainage. A possible explanation for this may stem from the presence of deep drainage canals that lead to lower water table depths compared to the rest of SEA. In this area, canals are on average 2 m deep (significantly deeper than the average canal depth elsewhere in the region) and in some cases extend multiple meters down to the underlying clay substrata (Suryadiputra et al., 2005). Such deep canals coupled with a lack of flow control structures have resulted in canal water levels that are shifted multiple meters below the ground surface (Vernimmen, Hooijer, Mulyadi, et al., 2020). Deep water levels within canals, in turn, may influence water table depths at further distances from the canals. In comparison, control structures such as weirs are now generally employed in other parts of the region (in part informed by the early failures of the ex-Mega Rice Project) aiming to maintain water table levels within 1 m of the ground surface (Lim et al., 2012). Accordingly, tracking of canal water levels is needed to better understand the impact of drainage density and canal layout on water table depths away from canals. Lidar measurements, previously used in tropical peatlands for mapping carbon stocks (Vernimmen, Hooijer, Akmalia, et al., 2020) and for estimating carbon losses from burn scars (Ballhorn et al., 2009; Simpson et al., 2016) are especially promising for measuring canal water levels (Rahman et al., 2017; Vernimmen, Hooijer, Mulyadi, et al., 2020). Widespread lidar measurements would complement the drainage metrics introduced in this study.

4.3 Potential applications of canal maps

In this study, we introduced a method for mapping drainage canals using satellite imagery and deep learning; our methodology is transferable to other geographic locations that are sensitive to drainage, such as temperate and boreal peatlands. Currently, drainage canals are less prevalent in other tropical peatlands such as those in the Congo and Amazon river basins, which have so far experienced less extensive land use change (Dargie et al., 2019; van Lent et al., 2019; Lilleskov et al., 2019). However, increasing economic pressure for timber extraction and oil palm, coupled with a dearth of protective regulations, indicate these basins are similarly vulnerable to the same path of peatland degradation as in SEA (Lilleskov et al., 2019). Long-term drying in European peatlands has similarly been attributed in part to anthropogenic drainage, and a renewed focus on rewetting via canal-blocking has emerged (Swindles et al.,

2019). Thus, there is a clear need to track the global expansion of peatland drainage. The growing availability of publically available, high-resolution satellite imagery, combined with our classification method, open the door for monitoring drainage canal development in global peatlands across both space and time.

The drainage density maps produced here can also be used towards representing drainage in modeling studies, both at individual sites and across larger areas. Recent investigations to simulate water table depth have relied on assumptions of drainage based on land use type to parametrize subsurface flow and boundary conditions in hydrologic models (e.g., (Mezbahuddin et al., 2015; Taufik et al., 2020)). Other recent studies have modeled fire risk in peatlands considering a wide range of factors (e.g., (Sloan et al., 2017; Sze & Lee, 2018)), but similarly have had to rely on land use metrics and road datasets as a proxies for drainage, due to the lack of regional drainage density information. Our dataset will facilitate more direct parametrization of drainage in both mechanistic and statistical modeling efforts.

In addition to drainage density, canal maps provide information about canal network shapes which, in conjunction with natural rivers, determine the carbon storage potential in peatlands by altering the shape of the water table (Cobb et al., 2017). The thickness of the vadose zone determines subsidence rates, so canal maps can provide information about which areas are likely to experience subsidence, as observed in Figure S4. Long-term peatland storage is also strongly governed by peat dome shape, which in turn is determined by boundary conditions. In drained systems, canal spacing limits the peat that can be preserved by waterlogging (Cobb et al., 2020), so canal maps are essential for determining the potential capacity for peat carbon storage. Accordingly, canal maps will be essential for determining not only carbon fluxes in the present, but also long-term carbon storage potential for years to come.

Over the past decade, there has been increasing interest in the potential of peatland hydrological restoration to reduce greenhouse gas emissions (Leifeld et al., 2019; Morecroft et al., 2019; Wilson et al., 2016). Although questions remain about the potential for overall reductions in greenhouse gases, due to compensating methane emissions (Hemes et al., 2018), the long term mitigation potential of rewetting via canal-blocking likely outweighs the increase in methane emissions (Günther et al., 2020). Thus, an understanding of drainage conditions, including canal mapping, should be a crucial component for identifying areas of peatland degradation. When combined with other datasets in peatlands such as remotely sensed soil moisture (Dadap et al., 2019), our maps may help peatland managers prioritize areas for hydrologic restoration. The results presented here further suggest that drainage canal maps could be used to more accurately represent peatland carbon emissions and hydrology, and therefore will serve as an important tool for protecting peatland ecosystems.

Acknowledgments and Data

The drainage canal maps developed in this study are available for download at [*will add link to data from Stanford digital repository, currently being setup with an ODC Attribution (ODC-BY) license for access without restrictions*]. Land use and and subsidence data used in this study are available from Miettinen et al. (2016) and Hoyt et al. (2020), respectively.

NCD was supported by NASA Headquarters under the NASA Earth and Space Science Fellowship Program – Grant 80NSSC18K1341. This work is supported by NSF under Award EAR-1923478 to AGK and CFH. This research was also supported by the National Research

Foundation (NRF), Prime Minister's Office, Singapore under its Campus for Research Excellence and Technological Enterprise (CREATE) program and Grant No. NRF2016-ITCOO1-021. The Center for Environmental Sensing and Modeling (CENSAM) is an interdisciplinary research group (IRG) of the Singapore MIT Alliance for Research and Technology (SMART). This research was also supported by the Swiss National Science Foundation under a Sinergia Grant.

References

Aldrian, E., & Dwi Susanto, R. (2003). Identification of three dominant rainfall regions within Indonesia and their relationship to sea surface temperature. *International Journal of Climatology*, *23*(12), 1435–1452. https://doi.org/10.1002/joc.950

Astiani, D., Burhanuddin, B., Curran, L. M., Mujiman, M., & Salim, R. (2017). Effects of Drainage Ditches on Water Table Level, Soil Conditions and Tree Growth of Degraded Peatland Forests in West Kalimantan. *Indonesian Journal of Forestry Research*, *4*(1), 15–25. https://doi.org/10.20886/ijfr.2017.4.1.15-25

Bader, C., Müller, M., Schulin, R., & Leifeld, J. (2018). Peat decomposability in managed organic soils in relation to land use, organic matter composition and temperature. *Biogeosciences*, *15*(3), 703–719. https://doi.org/10.5194/bg-15-703-2018

Ballhorn, U., Siegert, F., Mason, M., & Limin, S. (2009). Derivation of burn scar depths and estimation of carbon emissions with LIDAR in Indonesian peatlands. *Proceedings of the National Academy of Sciences of the United States of America*, *106*(50). https://doi.org/10.1073/pnas.0906457106

Carlson, K. M., Curran, L. M., Asner, G. P., Pittman, A. M., Trigg, S. N., & Marion Adeney, J. (2013). Carbon emissions from forest conversion by Kalimantan oil palm plantations. *Nature Climate Change*, *3*(3), 283–287. https://doi.org/10.1038/nclimate1702

Carlson, K. M., Goodman, L. K., & May-Tobin, C. C. (2015). Modeling relationships between water table depth and peat soil carbon loss in Southeast Asian plantations. *Environmental Research Letters*, *10*(7). https://doi.org/10.1088/1748-9326/10/7/074006

Cobb, A. R., Hoyt, A. M., Gandois, L., Eri, J., Dommain, R., Abu Salim, K., et al. (2017). How temporal patterns in rainfall determine the geomorphology and carbon fluxes of tropical peatlands. *Proceedings of the National Academy of Sciences*, *114*(26). https://doi.org/10.1073/pnas.1701090114

Cobb, A. R., Dommain, R., Tan, F., Heng, N. H. E. H., & Harvey, C. F. (2020). Carbon storage capacity of tropical peatlands in natural and artificial drainage networks. *Environmental Research Letters*.

Couwenberg, J., & Hooijer, A. (2013). Towards robust subsidence-based soil carbon emission factors for peat soils in south-east Asia , with special reference to oil palm plantations. *Mires and Peat*, *12*(1), 1–13.

Couwenberg, J., Dommain, R., & Joosten, H. (2010). Greenhouse gas fluxes from tropical peatlands in south-east Asia. *Global Change Biology*, *16*(6), 1715–1732. https://doi.org/10.1111/j.1365-2486.2009.02016.x

Dadap, N. C., Cobb, A. R., Hoyt, A. M., Harvey, C. F., & Konings, A. G. (2019). Satellite soil moisture observations predict burned area in Southeast Asian peatlands. *Environmental Research Letters*, *14*(9). https://doi.org/10.1088/1748-9326/ab3891

Dargie, G. C., Lawson, I. T., Rayden, T. J., Miles, L., Mitchard, E. T. A., Page, S. E., et al. (2019). Congo Basin peatlands: threats and conservation priorities. *Mitigation and Adaptation Strategies for Global Change*, *24*(4), 669–686. https://doi.org/10.1007/s11027-017-9774-8

Dohong, A., Aziz, A. A., & Dargusch, P. (2017). A review of the drivers of tropical peatland degradation in South-East Asia. *Land Use Policy*, *69*, 349–360. https://doi.org/10.1016/j.landusepol.2017.09.035

Dommain, R., Couwenberg, J., & Joosten, H. (2010). Hydrological self-regulation of domed peatlands in south-east Asia and consequences for conservation and restoration. *Mires and Peat*, *6*, 1–17.

Evans, C. D., Williamson, J. M., Kacaribu, F., Irawan, D., Suardiwerianto, Y., Hidayat, M. F., et al. (2019). Rates and spatial variability of peat subsidence in Acacia plantation and forest landscapes in Sumatra, Indonesia. *Geoderma*, *338*, 410–421. https://doi.org/10.1016/j.geoderma.2018.12.028

Field, R. D., Van Der Werf, G. R., & Shen, S. S. P. P. (2009). Human amplification of drought-induced biomass burning in Indonesia since 1960. *Nature Geoscience*, *2*(3), 185–188. https://doi.org/10.1038/ngeo443

Gandois, L., Hoyt, A. M., Mounier, S., Le Roux, G., Harvey, C. F., Claustres, A., et al. (2020). From Canals to the Coast: Dissolved Organic Matter and Trace Metal Composition in Rivers Draining Degraded Tropical

Peatlands in Indonesia. *Biogeosciences*, 1–23. https://doi.org/10.5194/bg-2019-253

Gorelick, N., Hancher, M., Dixon, M., Ilyushchenko, S., Thau, D., & Moore, R. (2017). Google Earth Engine: Planetary-scale geospatial analysis for everyone. *Remote Sensing of Environment*, *202*, 18–27. https://doi.org/10.1016/j.rse.2017.06.031

Günther, A., Barthelmes, A., Huth, V., Joosten, H., Jurasinski, G., Koebsch, F., & Couwenberg, J. (2020). Prompt rewetting of drained peatlands reduces climate warming despite methane emissions. *Nature Communications*, *11*(1), 1644. https://doi.org/10.1038/s41467-020-15499-z

Hemes, K. S., Chamberlain, S. D., Eichelmann, E., Knox, S. H., & Baldocchi, D. D. (2018). A Biogeochemical Compromise: The High Methane Cost of Sequestering Carbon in Restored Wetlands. *Geophysical Research Letters*, *45*(12), 6081–6091. https://doi.org/10.1029/2018GL077747

Hiraishi, T., Krug, T., Tanabe, K., Srivastava, N., Baasansuren, J., Fukuda, M., & Troxler, T. G. (2014). *2013 Supplement to the 2006 IPCC Guidelines for National Greenhouse Gas Inventories : Wetlands Task Force on National Greenhouse Gas Inventories*. Switzerland.

Hirano, T., Jauhiainen, J., Inoue, T., & Takahashi, H. (2009). Controls on the carbon balance of tropical peatlands. *Ecosystems*, *12*(6), 873–887. https://doi.org/10.1007/s10021-008-9209-1

Hirano, T., Kusin, K., Limin, S., & Osaki, M. (2015). Evapotranspiration of tropical peat swamp forests. *Global Change Biology*, *21*(5), 1914–1927. https://doi.org/10.1111/gcb.12653

Hooijer, A., Page, S., Canadell, J. G., Silvius, M., Kwadijk, J., Wösten, H., & Jauhiainen, J. (2010). Current and future CO 2 emissions from drained peatlands in Southeast Asia. *Biogeosciences*, *7*(5), 1505–1514. https://doi.org/10.5194/bg-7-1505-2010

Hooijer, A., Page, S., Jauhiainen, J., Lee, W. A., Lu, X. X., Idris, A., & Anshari, G. (2012). Subsidence and carbon loss in drained tropical peatlands. *Biogeosciences*, *9*(3), 1053–1071. https://doi.org/10.5194/bg-9-1053-2012

Houterman, J., & Ritzema, H. P. (2009). *Land and Water Management in the Ex-Mega Rice Project Area in Central Kalimantan. Technical Report No. 4, Master Plan for the Rehabilitation and Revitalisation of the Ex-Mega Rice Project Area, Central Kalimantan, Indonesia.*

Hoyt, A. M., Gandois, L., Eri, J., Kai, F. M., Harvey, C. F., & Cobb, A. R. (2019). CO2 emissions from an undrained tropical peatland: Interacting influences of temperature, shading and water table depth. *Global Change Biology*, *25*(9). https://doi.org/10.1111/gcb.14702

Hoyt, A. M., Chaussard, E., Seppalainen, S., & Harvey, C. (2020). Widespread Subsidence and Carbon Emissions across Southeast Asia Peatlands. *Nature Geoscience*, *13*, 435–440. https://doi.org/10.1038/s41561-020-0575-4

Jaenicke, J., Wösten, H., Budiman, A., & Siegert, F. (2010). Planning hydrological restoration of peatlands in Indonesia to mitigate carbon dioxide emissions. *Mitigation and Adaptation Strategies for Global Change*, *15*(3), 223–239. https://doi.org/10.1007/s11027-010-9214-5

Jauhiainen, J., & Silvennoinen, H. (2012). Diffusion GHG fluxes at tropical peatland drainage canal water surfaces. *Suo*, *63*(3–4), 93–105.

Jauhiainen, J., Takahashi, H., Heikkinen, J. E. P., Martikainen, P. J., & Vasander, H. (2005). Carbon fluxes from a tropical peat swamp forest floor. *Global Change Biology*, *11*(10), 1788–1797. https://doi.org/10.1111/j.1365-2486.2005.001031.x

Jauhiainen, J., Hooijer, A., & Page, S. E. (2012). Carbon dioxide emissions from an Acacia plantation on peatland in Sumatra, Indonesia. *Biogeosciences*, *9*(2), 617–630. https://doi.org/10.5194/bg-9-617-2012

Konecny, K., Ballhorn, U., Navratil, P., Jubanski, J., Page, S. E., Tansey, K., et al. (2016). Variable carbon losses from recurrent fires in drained tropical peatlands. *Global Change Biology*, *22*(4), 1469–1480. https://doi.org/10.1111/gcb.13186

Koplitz, S. N., Mickley, L. J., Marlier, M. E., Buonocore, J. J., Kim, P. S., Liu, T., et al. (2016). Public health impacts of the severe haze in Equatorial Asia in September-October 2015: Demonstration of a new framework for informing fire management strategies to reduce downwind smoke exposure. *Environmental Research Letters*, *11*(9), 094023. https://doi.org/10.1088/1748-9326/11/9/094023

Krizhevsky, A., Sutskever, I., & Hinton, G. E. (2017). ImageNet classification with deep convolutional neural networks. *Communications of the ACM*, *60*(6), 84–90. https://doi.org/10.1145/3065386

Kurnianto, S., Selker, J., Boone Kauffman, J., Murdiyarso, D., & Peterson, J. T. (2018, March 19). The influence of land-cover changes on the variability of saturated hydraulic conductivity in tropical peatlands. *Mitigation and Adaptation Strategies for Global Change*, pp. 1–21. https://doi.org/10.1007/s11027-018-9802-3

LeCun, Y., Bottou, L., Bengio, Y., & Haffner, P. (1998). Gradient-based learning applied to document recognition. *Proceedings of the IEEE*, *86*(11), 2278–2323. https://doi.org/10.1109/5.726791

Leifeld, J., & Menichetti, L. (2018). The underappreciated potential of peatlands in global climate change mitigation strategies. *Nature Communications*, *9*(1), 1071. https://doi.org/10.1038/s41467-018-03406-6

Leifeld, J., Wüst-Galley, C., & Page, S. (2019). Intact and managed peatland soils as a source and sink of GHGs from 1850 to 2100. *Nature Climate Change*, *9*(12), 945–947. https://doi.org/10.1038/s41558-019-0615-5

van Lent, J., Hergoualc'h, K., Verchot, L., Oenema, O., & van Groenigen, J. W. (2019). Greenhouse gas emissions along a peat swamp forest degradation gradient in the Peruvian Amazon: soil moisture and palm roots effects. *Mitigation and Adaptation Strategies for Global Change*, *24*(4), 625–643. https://doi.org/10.1007/s11027-018-9796-x

Lilleskov, E., McCullough, K., Hergoualc'h, K., del Castillo Torres, D., Chimner, R., Murdiyarso, D., et al. (2019). Is Indonesian peatland loss a cautionary tale for Peru? A two-country comparison of the magnitude and causes of tropical peatland degradation. *Mitigation and Adaptation Strategies for Global Change*, *24*(4), 591–623. https://doi.org/10.1007/s11027-018-9790-3

Lim, K. H., Lim, S. S., Parish, F., & Suharto, R. (2012). *RSPO Manual on Best Management Practices (BMPs) for Existing Oil Palm Cultivation on Peat*. Kuala Lumpur, Malaysia: RSPO.

Manoli, G., Meijide, A., Huth, N., Knohl, A., Kosugi, Y., Burlando, P., et al. (2018). Ecohydrological changes after tropical forest conversion to oil palm. *Environmental Research Letters*, *13*(6). https://doi.org/10.1088/1748-9326/aac54e

Mezbahuddin, M., Grant, R. F., & Hirano, T. (2015). How hydrology determines seasonal and interannual variations in water table depth, surface energy exchange, and water stress in a tropical peatland: Modeling versus measurements. *Journal of Geophysical Research: Biogeosciences*, *120*(11), 2132–2157. https://doi.org/10.1002/2015JG003005

Miettinen, J., Hooijer, A., Wang, J., Shi, C., & Liew, S. C. (2012). Peatland degradation and conversion sequences and interrelations in Sumatra. *Regional Environmental Change*, *12*(4), 729–737. https://doi.org/10.1007/s10113-012-0290-9

Miettinen, J., Shi, C., & Liew, S. C. (2016). Land cover distribution in the peatlands of Peninsular Malaysia, Sumatra and Borneo in 2015 with changes since 1990. *Global Ecology and Conservation*, *6*, 67–78. https://doi.org/10.1016/j.gecco.2016.02.004

Miettinen, J., Hooijer, A., Vernimmen, R., Liew, S. C., & Page, S. E. (2017). From carbon sink to carbon source: Extensive peat oxidation in insular Southeast Asia since 1990. *Environmental Research Letters*, *12*(2), 024014. https://doi.org/10.1088/1748-9326/aa5b6f

Moore, S., Evans, C. D., Page, S. E., Garnett, M. H., Jones, T. G., Freeman, C., et al. (2013). Deep instability of deforested tropical peatlands revealed by fluvial organic carbon fluxes. *Nature*, *493*(7434), 660–663. https://doi.org/10.1038/nature11818

Morecroft, M. D., Duffield, S., Harley, M., Pearce-Higgins, J. W., Stevens, N., Watts, O., & Whitaker, J. (2019). Measuring the success of climate change adaptation and mitigation in terrestrial ecosystems. *Science*, *366*(6471). https://doi.org/10.1126/science.aaw9256

Murdiyarso, D., Hergoualc'h, K., Verchot, L. V., Pittman, A. M., Soares-Filho, B. S., Asner, G. P., et al. (2010). Opportunities for reducing greenhouse gas emissions in tropical peatlands. *Proceedings of the National Academy of Sciences*, *107*(46), 19655–19660. https://doi.org/10.1073/pnas.0911966107

Oner, D., Koziński, M., Citraro, L., Dadap, N. C., Konings, A. G., & Fua, P. (*under review*). Promoting Connectivity of Network-Like Structures by Enforcing Region Separation. Submitted to: *IEEE Transactions on Pattern Analysis and Machine Intelligence*. Preprint available at: https://arxiv.org/abs/2009.07011.

Page, S. E., Siegert, F., Rieley, J. O., Boehm, H.-D. V., Jaya, A., & Limin, S. (2002). The amount of carbon released from peat and forest fires in Indonesia during 1997. *Nature*, *420*(6911), 61–65. https://doi.org/10.1038/nature01131

Page, S. E., Rieley, J. O., & Banks, C. J. (2011). Global and regional importance of the tropical peatland carbon pool. *Global Change Biology*, *17*(2), 798–818. https://doi.org/10.1111/j.1365-2486.2010.02279.x

Planet Team. (2017). Planet Application Program Interface: In Space for Life on Earth. San Francisco, CA.

Rahman, M. M., McDermid, G. J., Strack, M., & Lovitt, J. (2017). A New Method to Map Groundwater Table in Peatlands Using Unmanned Aerial Vehicles. *Remote Sensing*, *9*(10), 1057. https://doi.org/10.3390/rs9101057

Ronneberger, O., Fischer, P., & Brox, T. (2015). U-net: Convolutional networks for biomedical image segmentation. In *Lecture Notes in Computer Science (including subseries Lecture Notes in Artificial Intelligence and Lecture Notes in Bioinformatics)* (Vol. 9351, pp. 234–241). Springer Verlag. https://doi.org/10.1007/978-3-319-24574-4_28

Simpson, J. E., Wooster, M. J., Smith, T. E. L., Trivedi, M., Vernimmen, R. R. E., Dedi, R., et al. (2016). Tropical peatland burn depth and combustion heterogeneity assessed using uav photogrammetry and airborne LiDAR. *Remote Sensing*, *8*(12), 1000. https://doi.org/10.3390/rs8121000

Sinclair, A. L., Graham, L. L. B., Putra, E. I., Saharjo, B. H., Applegate, G., Grover, S. P., & Cochrane, M. A.

(2020). Effects of distance from canal and degradation history on peat bulk density in a degraded tropical peatland. *Science of the Total Environment*, *699*, 134199. https://doi.org/10.1016/j.scitotenv.2019.134199

Sloan, S., Locatelli, B., Wooster, M. J., & Gaveau, D. L. A. (2017). Fire activity in Borneo driven by industrial land conversion and drought during El Niño periods, 1982–2010. *Global Environmental Change*, *47*, 95–109. https://doi.org/10.1016/j.gloenvcha.2017.10.001

Suryadiputra, N., Dohong, A., Waspodo, R., Lubis, I., Hasudungan, F., & Wibisono, I. T. (2005). *A Guide to Blocking of Canals and Ditches in Conjunction with the Community*. *Wetlands International–Indonesia Programme*. Bogor.

Swindles, G. T., Morris, P. J., Mullan, D. J., Payne, R. J., Roland, T. P., Amesbury, M. J., et al. (2019). Widespread drying of European peatlands in recent centuries. *Nature Geoscience*, *12*(11), 922–928. https://doi.org/10.1038/s41561-019-0462-z

Sze, J. S., & Lee, J. S. H. (2018). Evaluating the social and environmental factors behind the 2015 extreme fire event in Sumatra, Indonesia. *Environmental Research Letters*. https://doi.org/10.1088/1748-9326/aaee1d

Taufik, M., Minasny, B., McBratney, A. B., Van Dam, J., Jones, P., & Van Lanen, H. (2020). Human-induced changes in Indonesia peatlands increase drought severity. *Environmental Research Letters*, (May).

Usup, A., Hashimoto, Y., Takahashi, H., & Hayasaka, H. (2004). Combustion and thermal characteristics of peat fire in tropical peatland in Central Kalimantan, Indonesia. *Tropics*, *14*, 1–19.

Vernimmen, R., Hooijer, A., Mulyadi, D., Setiawan, I., Pronk, M., & Yuherdha, A. T. (2020). A new method for rapid measurement of canal water table depth using airborne LiDAR, with application to drained peatlands in indonesia. *Water (Switzerland)*, *12*(5). https://doi.org/10.3390/w12051486

Vernimmen, R., Hooijer, A., Akmalia, R., Fitranatanegara, N., Mulyadi, D., Yuherdha, A., et al. (2020). Mapping deep peat carbon stock from a LiDAR based DTM and field measurements, with application to eastern Sumatra. *Carbon Balance and Management*, *15*(1), 4. https://doi.org/10.1186/s13021-020-00139-2

Warren, M., Hergoualc'h, K., Kauffman, J. B., Murdiyarso, D., & Kolka, R. (2017). An appraisal of Indonesia's immense peat carbon stock using national peatland maps: Uncertainties and potential losses from conversion. *Carbon Balance and Management*, *12*(1). https://doi.org/10.1186/s13021-017-0080-2

Wedeux, B., Dalponte, M., Schlund, M., Hagen, S., Cochrane, M., Graham, L., et al. (2020). Dynamics of a human-modified tropical peat swamp forest revealed by repeat lidar surveys. *Global Change Biology*. https://doi.org/10.1111/gcb.15108

Wells, J. A., Wilson, K. A., Abram, N. K., Nunn, M., Gaveau, D. L. A., Runting, R. K., et al. (2016, June 1). Rising floodwaters: Mapping impacts and perceptions of flooding in Indonesian Borneo. *Environmental Research Letters*. IOP Publishing. https://doi.org/10.1088/1748-9326/11/6/064016

van der Werf, G. R., Dempewolf, J., Trigg, S. N., Randerson, J. T., Kasibhatla, P. S., Giglio, L., et al. (2008). Climate regulation of fire emissions and deforestation in equatorial Asia. *Proceedings of the National Academy of Sciences*, *105*(51), 20350–20355. https://doi.org/10.1073/pnas.0803375105

Wiedemann, C., Heipke, C., Mayer, H., & Jamet, O. (1998). Empirical Evaluation Of Automatically Extracted Road Axes. *Empirical Evaluation Techniques in Computer Vision*, 172–187.

Wilson, D., Blain, D., Couwenberg, J., Evans, C. D., Murdiyarso, D., Page, S. E., et al. (2016). Greenhouse gas emission factors associated with rewetting of organic soils. *Mires and Peat*, *17*(04), 1–28. https://doi.org/10.19189/MaP.2016.OMB.222